Computerized Medical Imaging and Graphics 36 (2012) 356–365

Contents lists available at SciVerse ScienceDirect

Computerized Medical Imaging and Graphics

journal homepage: www.elsevier.com/locate/compmedimag

A hybrid deformable model for real-time surgical simulation

Bo Zhu, Lixu Gu*

Laboratory of Image Guided Surgery and Therapy, Med-X research Institute, Shanghai Jiao Tong University, China

ARTICLE INFO

Article history:
Received 23 August 2010
Received in revised form 24 February 2012
Accepted 2 March 2012

Keywords:
Virtual surgery simulation
Deformable modeling
Boundary element method
Physical simulation

ABSTRACT

Modeling organ deformation in real remains a challenge in virtual minimally invasive (MIS) surgery simulation. In this paper, we propose a new hybrid deformable model to simulate deformable organs in the real-time surgical training system. Our hybrid model uses boundary element method (BEM) to compute global deformation based on a coarse surface mesh and uses a mass-spring model to simulate the dynamic behaviors of soft tissue interacting with surgical instruments. The simulation result is coupled with a high-resolution rendering mesh through a particle surface interpolation algorithm. Accurate visual and haptic feedbacks are provided in real time and temporal behaviors of biological soft tissues including viscosity and creeping are modeled as well. We prove our model to be suitable to work in complex virtual surgical environment by integrating it into a MIS training system. The hybrid model is evaluated with respect to efficiency, accuracy and robustness by a series of experiments.

1. Introduction

1.1. Background

Interactive surgery simulation technique plays an important role in today's medical education system. Virtual reality (VR) and surgical simulators can provide the opportunity to expose each surgical resident to a wider surgical experience and to make the training more uniform. Over the past decades, training systems based on VR technology for different types of surgeries have been developed, including facial plastic [19], cataract [7], neurosurgery [38], knee [5], laparoscope [40], hysteroscopy [41], and bone dissection [21]. Among these, training systems for minimally invasive surgery (MIS) have drawn a lot of attention. MIS is advantageous over other open surgeries for the smaller wound and less pain after operation. But it is much more difficult for a surgeon to operate based on the images provided by a laparoscopic camera in MIS than in a common open surgical situs. So a pre-operative training for a surgeon to adapt the anatomic knowledge to the laparoscopic environment, to practice manipulating surgical instruments with constraint degrees of freedom, and to get a sense of depth and direction in the new perspective is very necessary.

A variety of computational physics methods have been developed for realistically modeling the virtual surgery environment [4,29,31,32] and the user interactions, including the collision detection and response between soft tissues and instruments [40], deformation of organs in contact with surgical instruments [45], surgical operations including needle insertion [6], cutting and sewing [42]. A fast and robust deformable model continuously providing visual and haptic feedback to users is essential to the surgery training systems. There are four basic requirements for a deformable model used in real-time MIS simulation: accuracy, efficiency, robustness, and easiness to integrate into the system. First, in contrast to deformable models used in video games and animations, the purpose of such models in medical simulation is to model the behaviors of realistic biological tissues. The deformation should be controlled by real material parameters (Poisson Ratio and Young's Modulus) taken from biomechanics experiments instead of intuitively adjusted parameters. Some specific deformation effects of biological soft tissues, such as viscous response and free vibration, need to be simulated too. Second, the model needs to be fast enough to provide results within 1/30 to 1/50 s. This eliminates most of the standard methods developed in computational physics, which are too slow to be used in real-time applications. Third, the model needs to be robust to provide results under large deformations and in large timesteps. Fourth, the model should be easy to integrate into a complex MIS simulator. In a typical virtual surgical environment, objects with different material properties, phases, geometry shapes and data representations are often combined together, and different types of interactions and responses between them need to be handled together.

1.2. Related works

Simulation of deformable objects becomes a hot topic in biomedical engineering, computational physics, and computer graphics. A lot of methods have been proposed over the past decades, and we refer the reader to the survey [27] for an overview.

* Corresponding author. Tel.: +86 21 34204137.
E-mail address: gulixu@sjtu.edu.cn (L. Gu).

0895-6111/$ – see front matter © 2012 Elsevier Ltd. All rights reserved.
doi:10.1016/j.compmedimag.2012.03.001

Deformable models can be classified into two categories: physics-based and non physics-based. Physics-based methods are based on continuum mechanics, and could get accurate simulation results by directly solving the partial differential equations (PDEs) using numerical methods. Some of the prevailing methods include the finite element method (FEM) [28], boundary element method (BEM) [12], point-based method [24], and reduced model [11]. Non physical models use intuitive methods instead of solving PDE. For example, the mass-spring model [35] uses point masses connected by a network of springs to represent continuous material, and meshless shape matching model [23] computes deformations based on geometry shapes.

There are some advances in real-time modeling of deformable objects in medical simulation and computer graphics. Müller et al. [22] use corotational FEM to simulate large deformations with implicit integration in real time, and similar methods are used in simulating biological soft tissues in [28]. In [26], cube meshes are used instead of tetrahedron meshes to simplify the matrix computation in real-time FEM simulation. In [12] and [14], boundary element method, which focuses on the surface, is proposed by James and Pai to model deformable objects in interactive applications. Reduced models [13] divide the deformation into different modes and model the global deformations with very low computation cost. Meshless methods use discrete points instead of tetrahedron mesh to represent continuum, and solve the PDE by employing interpolation methods such as moving least squares (MLS) [24] or smoothed particle hydrodynamics (SPH) [20]. Non-physical methods can also be pushed to accurate modeling by carefully adjusting the parameters and adding physical constraints. In [35], additional volume conservation constraints are combined with mass-spring model to simulate incompressible material. In [8], mass-spring model with parameters measured in experiments is used to simulate the local deformation of anatomical organs in surgical environment.

BEM is a physics accurate method restricting the computation domain on boundaries. It computes the deformation by numerically solving the boundary integration equation on a surface mesh. Because the simulation is only on boundary, no computation resource is wasted in updating the volume and therefore the efficiency is very high. James and Pai achieved to simulate deformable objects using BEM in interactive application ArtDefo [12]. One problem of BEM is its scalability, because the global matrix of BEM is dense and asymmetric and needs to update in each timestep. To improve this, James and Pai [14] use multi-resolution Green Function to accelerate the computation of BEM matrix. BEM are also used in virtual surgery to model the deformation of organs. Kim et al. [16] use local surface mesh subdivision and interpolation to enhance the details of contact areas in surgical simulation. Zhu et al. [43] use a finite state machine to estimate the stressing state of soft body in surgical simulation. Wang et al. [39] integrate BEM with cutting algorithm, which extends the applications of BEM in surgical simulation.

Reduced deformable models [1,11,13] also draw a lot of attentions in real-time deformable modeling. In reduced models, modes of global deformation are computed using modal analyzing [11], dynamics response textures [13] or non-linear techniques [1]. The deformation is then embedded into a standard rigid body dynamics simulator and both systems evolve over time. In our coupling method, we use BEM computation and mass-spring model to couple the precise global deformation information with a time evolving model.

1.3. Our approach

We propose a new hybrid deformable model for real-time surgical simulation. Our model is able to provide visually accurate and robust results for the surgical trainees and is able to work efficiently in a real-time MIS simulator. The basic idea is to couple the boundary element method into a mass-spring constraint model. Instead of just solving the boundary value problem of linear elasticity as in standard BEM, BEM is used to compute the global deformation which is regarded as target positions for mass particles in a mass-spring model. And the global deformation shape of mass-spring model is controlled by the target positions. By tuning the stiffness and damping parameters of spring, we are also able to model the temporal and detailed deformation behaviors of the organ.

Our hybrid model adds the ability of modeling temporal deformable behavior to the standard BEM. In essence, simulating deformable objects using BEM is solving a boundary value problem (BVP) which is unrelated to the time variable. BEM simulates the deformation behavior of perfect linear elastic material based on the current boundary displacement and traction conditions of the object. It cannot model the non-linear deformation behavior related to time including viscous or damping effect. We solve this problem by integrating BEM into a dynamic deformable model driven by an extra mass-spring model. This turns the pure boundary value problem into a initial value problem which is easy to solve.

2. Surface modeling from medical data

We use three different types of data structures to represent the surface of a deformable object: a high-resolution polygon mesh for rendering, a low-resolution polygon mesh for physics computation, and a particle sampled surface to synchronize the two meshes (as in Fig. 1). The two surface meshes are generated from raw medical data using standard surface reconstruction algorithm, and the particle surface is generated by sampling the coarse triangle mesh. Different surfaces are synchronized using fast mesh-particle interpolation.

Both fine and coarse polygon meshes are extracted directly from segmented medical data in DICOM format by employing marching cube algorithm. The geometry details are preserved in the fine surface, while the coarse surface is smoothed to avoid potential numerical errors caused by bad shapes of small triangles in simulation steps.

Particle surface is a kind of surface represented by discrete sampling particles without any topology information. It was used in [2] to handle the interactions between rigid objects and granular particles. In [33,45], it is proved to be an efficient and uniform way to handle the collisions and contacts between objects with different physics models. Similarly, particle surface is used in our method to handle collision detections and responses between deformable objects and other elements such as scalpel models in surgical environments and can be integrated seamlessly in our point based MIS simulation framework [44]. We use the particle surface extraction method in [45] to construct the particle surface as in Fig. 1. This particle surface bridge the coarse and fine polygon meshes in simulation.

3. Hybrid deformable model

3.1. Model overview

As in Fig. 2, our hybrid method contains three main parts: a static BEM-based elasticity solver, a dynamic mass-spring model, and a particle surface interpolation algorithm. In the preprocessing stage, the global deformation matrix of BEM is initialized using the coarse geometrical mesh and the measured linear elastic material parameters (Poisson Ratio and Young's Modulus). Other experimented parameters including the spring parameters are also loaded in this stage. In runtime computing, the physical accurate global

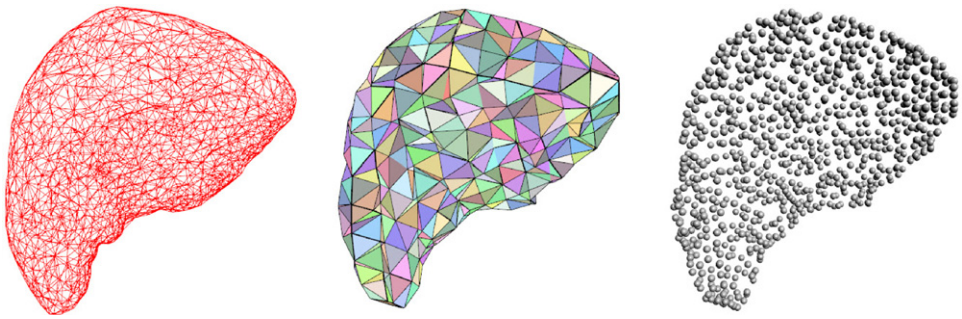

Fig. 1. High-resolution mesh (left), low-resolution mesh (middle) and particle surface (right) with $\rho = 1$ of a liver model reconstructed from the same medical data.

deformations are computed in the BEM solver according to the current boundary condition, and then served as target positions for the dynamic mass-spring model. In the simulation loop, mass points on particle surface are drawn toward these well-defined goal positions by the connecting springs, and the inaccurate and instable problems in standard mass-spring model are eliminated.

By adjusting the spring parameters, realistic dynamic deformation responses of biological tissues like the viscosity and creeping can be simulated in real time without adding the complexity of the problem. With the hybrid computed surface deformations on coarse mesh and particle surface, the shape of the fine visualization surface is synchronized by using a surface particle interpolation algorithm, and accurate visual and haptic feedbacks are provided in runtime. The interactions between the deformable model and VR environment, including collisions, contacts and dynamic simulations, are handled by the particle surface using point-based techniques.

3.2. Computing global deformation using boundary element method

The BEM model computes physical accurate global deformations. It contains two stages: the pre-processing stage and the runtime computation stage. In the pre-processing stage, a global deformation matrix with $3N \times 3N$ elements is constructed from the coarse polygon surface with N elements. Young's Modulus and Poisson Ratio measured from experiments are used to set up the global matrix based on linear elastic theory. In runtime computation, surface forces exerted on the object are regarded as a vector with 3N elements and multiplied with the global matrix to get the target position of global deformations (Fig. 2).

3.2.1. Pre-computing global deformation matrix

The computation of global deformation matrix based on linear elastic theory plays a central role in BEM simulation. Different

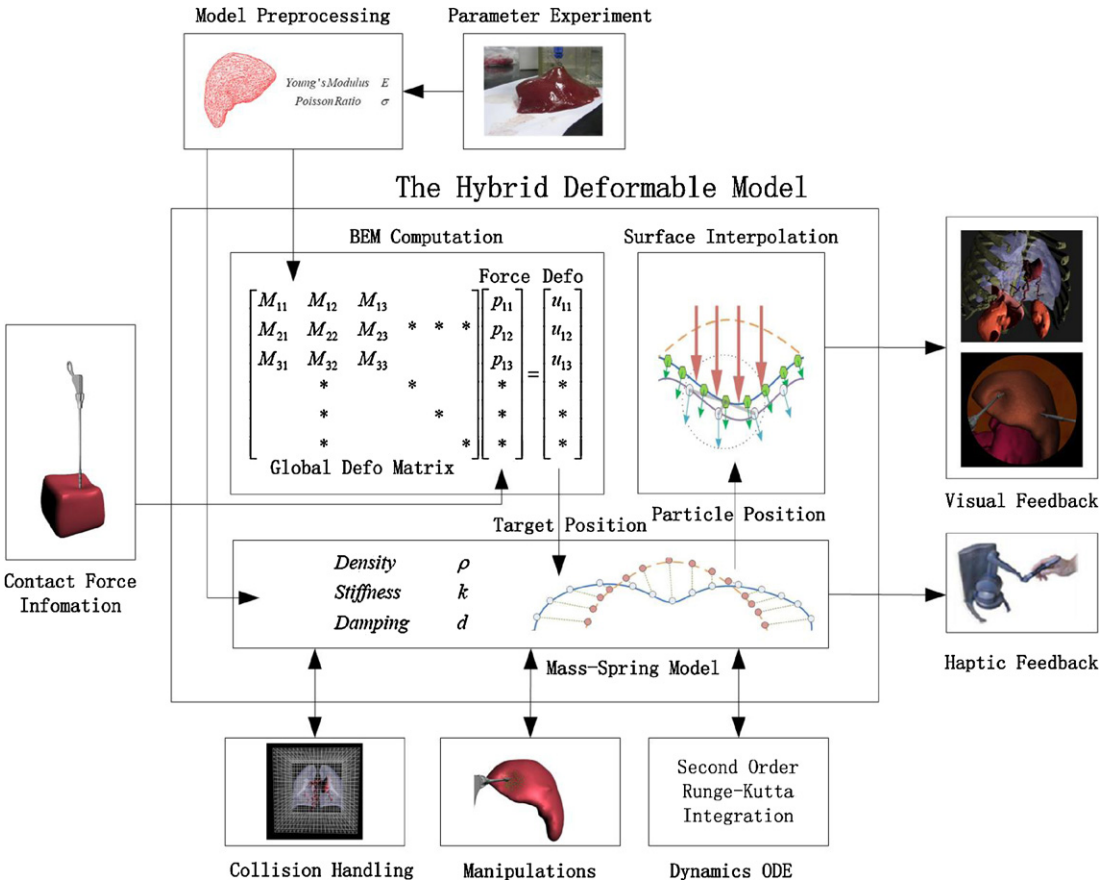

Fig. 2. Overview of the hybrid method for real time simulating organ deformations in virtual surgery.

from the sparse and symmetric matrix used in FEM, matrix used in BEM is dense and asymmetric. We extend the standard method in [12] and [16] for the computation of the global matrix. Further implementation details can be found in [3,9,30].

The physics model of BEM is based on Navier's equation of isotropic linear material, which has the form

$$\lambda \mathbf{u}_{k,ki} + G(\mathbf{u}_{i,jj} + \mathbf{u}_{j,ij}) + \mathbf{f}i = 0 \quad (i, j, k = 1, 2, 3) \tag{1}$$

Eq. (1) has a tensor formulation in which i, j, k denotes the three directions in xyz coordinate systems, $\mathbf{u}$ is displacement and $\mathbf{f}$ represents volume force. Then Green–Gauss theorem and the Kelvin fundamental solutions of linear elastostatic problem is used to convert Eq. (1) to an integral equation defined on the boundary of domain Ω,

$$\mathbf{C}_{lk}\mathbf{u}_k^i + \int_\Omega \mathbf{p}_{lk}^* \mathbf{u}_k d\Gamma = \int_\Gamma u_{lk}^* \mathbf{p}_k d\Gamma + \int_\Omega u_{lk}^* \mathbf{f}_k d\Gamma \quad (l, k = 1, 2, 3) \tag{2}$$

in which $\mathbf{C}_{lk}$ is a rank 2 tensor related to the smoothness of surface, here we use $\mathbf{C}_{lk} = (1/2)\delta_{lk}$. Γ is surface boundary and Ω is volume domain. In our method, we can take $\mathbf{f}_k = 0$ so the integral term of volume force could be omitted. $\mathbf{p}_{lk}^*$ and $\mathbf{u}_{lk}^*$ are Kelvin fundamental solutions for tractions and displacements. As for point P and Q on the surface, Kelvin fundamental solutions has the form

$$\mathbf{u}_{lk}^*(P, Q) = \frac{1}{16\pi(1-\upsilon)Gr}[(3-4\upsilon)\delta_{ij} + r_{,l}r_{,k}] \tag{3}$$

$$\mathbf{p}_{lk}^*(P, Q\prime) = -\frac{1}{8\pi(1-\upsilon)r^2}\left\{\frac{\partial r}{\partial n}[(1-2\upsilon)\delta_{lk} + 3r_{,l}r_{,k}] - (1-2\upsilon)(r_{,l}n_k - r_{,k}n_l)\right\} \tag{4}$$

Then the boundary integral equation is numerical discretized and written in a matrix formulation

$$\mathbf{C}\mathbf{u}_i + \sum_{j=1}^{N}\left(\int_{\Gamma_j}\mathbf{p}^* d\Gamma\right)\mathbf{u}_j = \sum_{j=1}^{N}\left(\int_{\Gamma_j}\mathbf{u}^* d\Gamma\right)\mathbf{p}_j \quad (i = 1, \cdots, n) \tag{5}$$

in which $\mathbf{C}$ and two integration term are 3×3 matrixes, $\mathbf{u}_i$, $\mathbf{u}_j$, $\mathbf{p}_j$ are 3×1 vectors. As in [12] and [16], we take

$$\mathbf{H}_{ij} = \int_{\Gamma_j}\mathbf{p}^* d\Gamma + \mathbf{C}\delta_{ij} \tag{6}$$

$$\mathbf{G}_{ij} = \int_{\Gamma_j}\mathbf{u}^* d\Gamma \tag{7}$$

To compute the integral term in $\mathbf{H}_{ij}$ and $\mathbf{G}_{ij}$, Gauss integration method is employed on surface element i and j. Substituting Kelvin fundamental solutions into Gauss integration formula, we get

$$\mathbf{H}_{ij} = |S_j|\omega_k \sum_{k=1}^{7}\mathbf{u}_{ij}(P, Q_k) \tag{8}$$

$$\mathbf{G}_{ij} = |S_j|\omega_k \sum_{k=1}^{7}\mathbf{p}_{ij}(P, Q_k) \tag{9}$$

where S_j is the area of element j, ω_k are Gauss coefficients and P, Q are sampled points on the triangle surface. In our implementation we sample 7 points for each element. Then we get the linear equation system

$$\sum_{j=1}^{N}\mathbf{H}_{ij}\mathbf{u}_j = \sum_{j=1}^{N}\mathbf{G}_{ij}\mathbf{p}_j \quad (i = 1, \cdots, N) \tag{10}$$

More intuitively, (10) is rewritten as

$$\mathbf{HU} = \mathbf{GP} \tag{11}$$

$\mathbf{H}$ and $\mathbf{G}$ are $3N \times 3N$ matrixes, each containing $N \times N$ submatrixes $\mathbf{H}_{ij}$ and $\mathbf{G}_{ij}$. $\mathbf{U}$ and $\mathbf{P}$ are $1 \times 3N$ vectors composed of displacement and traction vectors of N surface elements. Then the global deformation $\mathbf{U}$ is computed as

$$\mathbf{U} = \mathbf{H}^{-1}\mathbf{GP} = \mathbf{MP} \tag{12}$$

where $\mathbf{M}$ is the global deformation matrix.

3.2.2. Runtime updating the target positions

With the matrix $\mathbf{M}$ computed in the pre-processing stage, we can get the global deformation of each element by simply multiplying $\mathbf{M}$ with surface traction vector $\mathbf{P}$. Because $\mathbf{M}$ is constant in runtime, the computation time only depends on the number of non-zero terms in $\mathbf{P}$, which means the update time is proportional to the influence area of external force. However, to restrict the contact force within a few surface elements will cause the artificial effects in simulation. As for real elastic material, pressure is distributed smoothly over a finite surface area, and considering pressure as a single element will cause inconsistencies.

In our method, we use pressure mask technique proposed in [12] and [8] to avoid this artificial phenomenon. The basic idea is to use a scalar function (called "mask function") to distribute the pressure on a single surface element to all the elements in a finite area. As for a surface element i under pressure $\mathbf{f}$, k nearest neighbor elements with topological distance h are firstly searched by employing breadth first search algorithm, then pressure on neighbor j is computed as $\mathbf{f} \cdot W(|x_j - x_i|, h)$. The mask function $W(r, h)$ here is a normalized symmetric function with compact support which is very similar to the kernel function used in SPH [20,33,17]. In BEM simulation, the shape of mask function directly influences the shape of local deformation detail. To realistically simulate the local deformation shapes of biological tissue, we choose the mask function experimentally as

$$W(r, h) = \begin{cases} \dfrac{e^{-r^2}}{\pi^{3/2}h^3} & r < h \\ 0 & \text{others} \end{cases} \tag{13}$$

The support field h in mask function also influences the deformation effects. We can simulate large scale deformations by simply increasing the support field h or equivalently, the mask scale, which is the proportion of neighbor number to the total surface element number (Fig. 3).

The mask function is only applied to enhance the smoothness and authenticity of local deformation details, which has no influence on global deformation effects. In some cases where local details are not noticeable, the support field h of mask function can be decreased to ensure the computation efficiency. But for most MIS applications where local details are important, it is necessary to use mask function to enhance deformation details at the expense of such extra computational cost.

3.3. Coupling with mass-spring model

BEM solves the deformation by taking new boundary conditions in each timestep. More specifically, it takes tractions or displacements of each surface element as input and computes the unknown quantities by solving a linear equation system. This process is time independent, which means in each timestep $\mathbf{M}$ is updated according only to the new boundary conditions but not the size of timestep. Comparing to solving a BVP, we use a different hybrid method to convert it to an initial value problem. Instead of updating the global deformation matrix each time, we couple the BEM computation with a mass-spring model which can evolve temporally (Fig. 4).

Global deformations are regarded as target positions for each surface point, and the current position and target position of each surface point are linked with a mass-less spring. The movements of the surface points are driven by the elastic force of the connecting

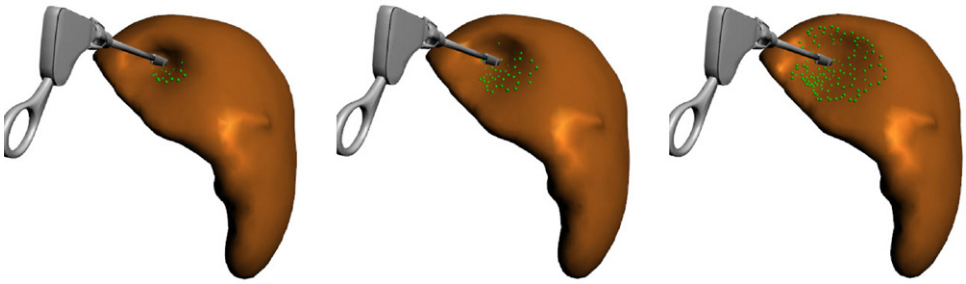

Fig. 3. Deformation of liver model with different mask scale: 0.01 (left), 0.02 (middle) and 0.05 (right).

spring toward the target position. In each time step, target positions are re-computed using the global deformation matrix according to the current external forces.

The dynamics of surface elements satisfies Newton's second law

$$\dot{\mathbf{v}} = \frac{\mathbf{f}(\mathbf{x}, \mathbf{v})}{m} \tag{14}$$

The spring forces acting on a surface element include elastic force and damping force. Elastic force is computed as

$$\mathbf{f}_{\text{elastic}} = k\frac{\mathbf{x}_{\text{target}} - \mathbf{x}_{\text{current}}}{|\mathbf{x}_{\text{target}} - \mathbf{x}_{\text{current}}|}(|\mathbf{x}_{\text{target}} - \mathbf{x}_{\text{current}}| - l_0) \tag{15}$$

where k is the stiffness coefficient and l_0 is the length of spring. We take $l_0 = 0$ in our model. Damping force is computed as

$$\mathbf{f}_{\text{damp}} = d(\mathbf{v}_{\text{target}} - \mathbf{v}_{\text{current}})\frac{\mathbf{x}_{\text{target}} - \mathbf{x}_{\text{current}}}{|\mathbf{x}_{\text{target}} - \mathbf{x}_{\text{current}}|} \tag{16}$$

in which d is the damping coefficient and $\mathbf{v}_{\text{target}}$ and $\mathbf{v}_{\text{current}}$ are the velocities of the target point and surface point. For the BEM model is only related to boundary force condition and irrelevant to time, the velocity of the target point $\mathbf{v}_{\text{target}}$ is always zero here.

In each time step, the target positions are updated by BEM computation, and a second order Runge–Kutta integration scheme is applied to update the new velocity and positions of each surface point (Table 1).

By coupling the BEM model with mass-spring model, five parameters are used in our hybrid model to simulate deformation of soft body: Young's Modulus E, Poisson's Ratio σ, density ρ, stiffness k and damping d. With the extra three spring parameters, our model provides ability to simulate more complex deformation phenomenon varying with time such as soft tissue with high viscosity or slow elastic recovery by adjusting the spring coefficients k and d and the material density ρ. For realistically surgical simulation, the

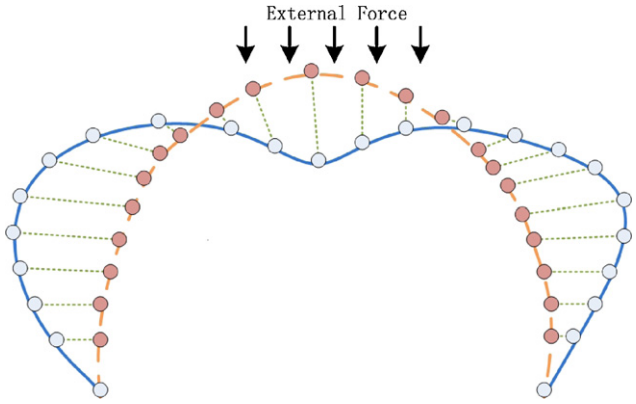

Fig. 4. The global deformations are computed using BEM and served as target positions (gray), the mass points on particle surface (red) are pulled toward the accurate deformation shapes (blue lines) by connecting springs (dotted lines). (For interpretation of the references to color in this figure legend, the reader is referred to the web version of the article.)

Table 1
Parameters of the hybrid model.

Parameters	Value range
Young's Modulus E (kPa)	100–110
Poisson's ratio σ	0.46–0.5
Density ρ (g cm^{-3})	1.0–1.1
Stiffness k	0.2–0.6
Damping d	0.3–0.8

value ranges of these parameters are measured by biomechanical experiments on samples of porcine kidney and liver. We determine E and σ by measuring the strain–stress relationship of soft tissue samples similar to the method used in [16]. Density is assumed to be constant within the tissue sample and is determined by measuring its mass and volume. The spring coefficients are then determined empirically to match the temporal responding deformations of the experimented real biological organs.

3.4. Integration into MIS simulator

In this section we show how to provide plausible feedback visually and haptically with our hybrid model in a virtual surgical environment. It includes the interpolation algorithm from the coarse BEM surface to the fine rendering surface, collision handling with surgical instruments in an interactive environment, and continuous feedback force computation. Point-based simulation techniques in [44] are used to accelerate the collision and haptic computation process of the MIS simulator.

3.4.1. Surface interpolation for rendering

In our hybrid deformable model, physics computation and visual rendering are separated and based on meshes with different resolutions. A fast interpolation algorithm is needed to synchronize the deformation of two surfaces together in one frame. In point-based simulations, interpolation algorithms are widely used in binding physics elements and rendering surfaces together [17,24], and the displacement of a surface vertex is determined by the weighted sum of the displacements of its neighbor physics points within radius h. We use the interpolation formation similar to [44] couple the two surfaces. The difference is that [44] takes volume particle positions as input and here we take positions of surface particles. The coupling method is based on interpolation between vertexes of rendering surface and points on particle surface. A kernel function is used to sum up the weighted displacements of neighbor points on particle surface and this sum is regarded as the displacement of the surface vertex:

$$\mathbf{u}_i^r = \frac{\sum_j W(\mathbf{x}_i - \mathbf{x}_j, h)\mathbf{u}_j^p}{\sum_j W(\mathbf{x}_i - \mathbf{x}_j, h)} \tag{17}$$

in which $\mathbf{u}_i^r$ is the displacement of surface rendering vertex and $\mathbf{u}_j^p$ is the displacement of its neighbor surface particles (Fig. 5). Here

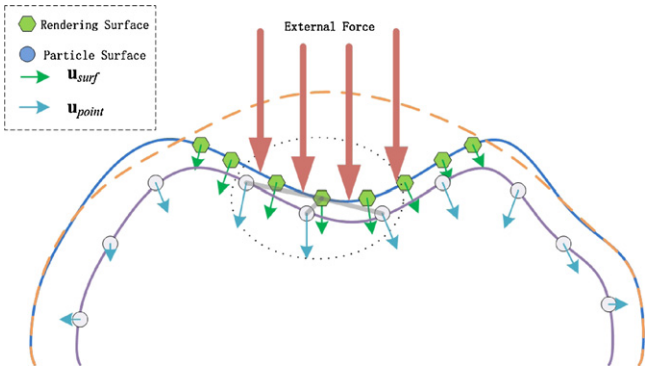

Fig. 5. Deformation of rendering surface (blue line with green points) is computed by interpolating the pre-defined neighbors on particle surface (white points on purple line). (For interpretation of the references to color in this figure legend, the reader is referred to the web version of the article.)

we use the spiky kernel function commonly used in SPH method to get a smoothed interpolation result:

$$W(h,r) = \begin{cases} \frac{15}{\pi h^6}(h-r)^3 & h < r \\ 0 & \text{others} \end{cases} \quad (18)$$

A high resolution surface can be controlled by a small number of particles on particle surface. But this method will cause the detail loss problem when the ratio of vertex numbers of the two surface $N_{\text{rendering}}/N_{\text{particle}}$ is too large, which can affect the visual results of deformation.

3.4.2. Collision detection and response in uniform grid

In our method, particle surface is used to handling collisions between deformable organs and other objects in the surgical environment. We use the uniform grid method in [45] to detect collisions between organs and instruments in the surgical environment. The algorithm subdivides the space into an array of aligned voxels with index in three dimensions. Then the elements of objects are put into these voxels, which can be visited efficiently in the array. This is similar to spatial hashing [34], in which different types of materials, such as soft bodies, rigid bodies and even fluids, can be handled in a unified way with high efficiency (Fig. 6).

3.4.3. Haptic feedback

After detecting collisions between anatomical organs and surgical instruments, a continuous response force needs to be computed and provided to the trainee with haptic devices. In order to get a smoothed force feedback, mask function used in BEM simulation is employed again to smooth the spring forces within the contact surface area. In experiment 4 we demonstrate that our model can provide accurate and continuous haptic feedback in real-time. In our MIS simulator, the haptic computation modular is integrated with Phantom haptic device. Trainees can use Phantom to manipulate the virtual instruments interacting with the deformable organs and feel the haptic feedback via the stylus immediately.

4. Experiments and evaluation

In this section we evaluate our hybrid deformable model by a series of experiments with respect to accuracy, efficiency and robustness. A MIS training system integrated with our hybrid model is presented in the last. Our model is implemented in C++ and rendered using OpenGL. All the experiments were carried out on a 2.26 GHz Pentium M notebook PC with GeForce 9650M graphics card and 2 GB of memory.

4.1. Accuracy

To evaluate the ability of the hybrid method to model real biological tissues, a set of experiments have been conducted to test if the approach can simulate the typical soft tissue behavior. First, like the standard BEM model, our model models the properties of linear elastic material including incompressibility and rigidness by setting values of Poisson Ratio and Young's Modulus in the pre-computing stage. As shown in Fig. 7, the sides of soft body bulge (pic. 1, 2, 3) and shrink (4, 5, 6) to conserve volume (with $\sigma = 0.47$) interacting with a scalpel and a nipple. Our hybrid method can simulate this deformation and provide the correct visual effects in real-time.

In addition to simulating the static deformed shapes of soft body by solving boundary value problem using standard BEM, our hybrid method is able to simulate dynamic deformation response of soft tissue when interacting with surgical instruments. These phenomena, including viscous response, damped vibration after external force removed, and material creeping under pressure, are important in realistically simulating biological organs and tissues. In our model, these deformation behaviors are simulated by adjusting the stiffness and damping parameters and coupling the dynamic effects with the static global deformation.

As in Fig. 8, same external pressures are exerted on three soft bodies (the first picture) with the same Young's Modulus and Poisson Ratio but different viscosity. After the external forces are

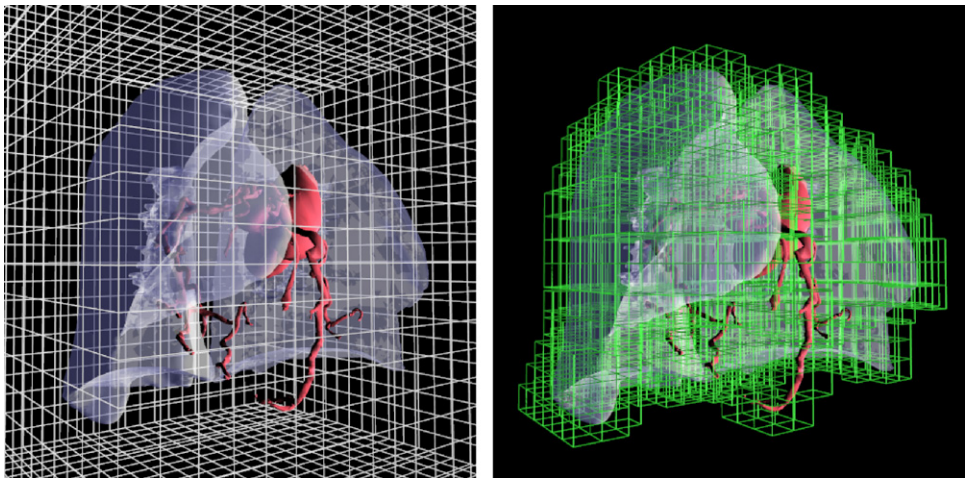

Fig. 6. The uniform grid subdivides the space into N^3 voxels (left), and the voxels containing the surface particles are updated in each time step (right).

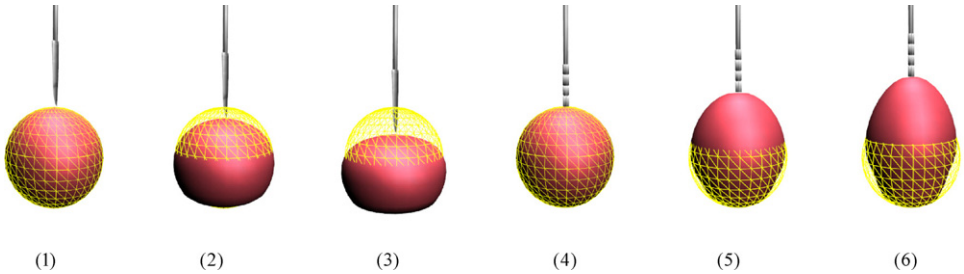

Fig. 7. Volume conserving deformation ($\sigma = 0.47$) of an elastic sphere under pressure (Picture 1,2,3) and dragging force (Picture 4,5,6), comparing with the rest shape (yellow mesh). (For interpretation of the references to color in this figure legend, the reader is referred to the web version of the article.)

Fig. 8. Different deformation responses with high (red), medium (ochre) and low (brown) viscosity. (For interpretation of the references to color in this figure legend, the reader is referred to the web version of the article.)

removed, different deformation responses are simulated: the body with low viscosity recovers to the initial shape quickly (the first object in the second picture), while the one with high viscosity (the third) restores very slow. This process can be adjusted by spring parameters in runtime.

Organ vibration after the target organ is grabbed or stabbed by surgical instruments is another noticeable phenomenon in surgical simulation, and some previous work has been done to simulate this process realistically [1,13]). Simulating the vibration process also depends on the stiffness and damping parameters of mass-spring model. Different vibration modes are tuned by independently adjusting stiffness coefficient k (Chart 1 in Fig. 9) and damping coefficient d (Chart 2 in Fig. 9). Vibration modes with different viscous property could be simulated by combined the two

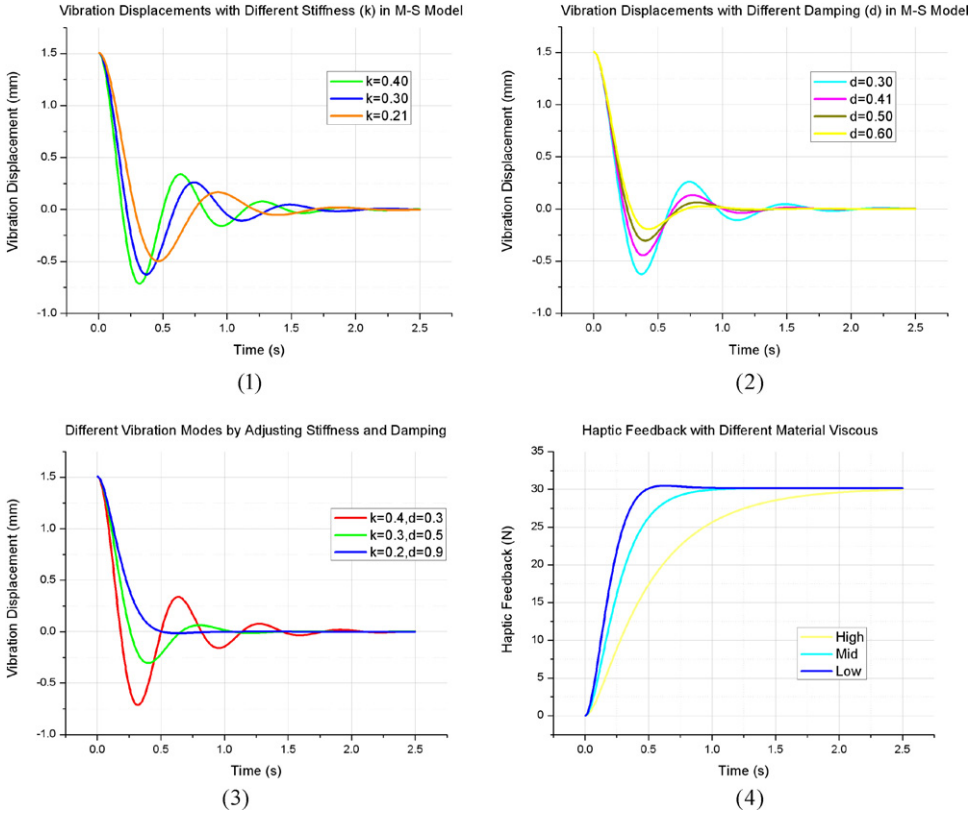

Fig. 9. Dynamic vibration modes with different spring parameters (Chart 1,2,3) and haptic feedback with different material viscosity.

Table 2
Time and memory performance of the hybrid model.

Model	Matrix size (Mb)	Pre-computation time (s)		BEM (ms)	Hybrid update (ms)	Overall (ms)
		H&G	M			
Model 1	2.77	0.61	0.44	0.63	0.36	0.99
Model 2	21.10	4.56	10.09	1.75	1.07	2.82
Model 3	44.93	9.83	31.67	2.53	1.64	4.17

parameters together (Chart 3 in Fig. 9). When a viscous tissue is constantly pushed by an instrument, the haptic feedback grows slowly and smoothly reaches the maximum stress value with material creeping [8]. In the creeping test, we simulate this phenomenon and record the resulting feedback force as a function of time. As illustrated in Chart 4 in Fig. 9, organ with lowest viscosity has the highest response force rate. And this result is similar to the creeping measurements obtained from real biological tissues [10,18].

4.2. Efficiency

We evaluate the performance of our hybrid deformable model in the aspects of memory and time cost. The time cost in one simulation step includes BEM computation on coarse mesh, mass-spring constraints and surface interpolation. In Table 2, we test three models with different surface resolutions ranging from 200 to 1200 surface vertexes. The items for comparison include the global deformation matrix size, pre-computation time (including computing matrix H & G, and inverse of H), BEM updating time, hybrid updating time (only for hybrid model) and the total time are, respectively, compared. It can be seen from the table that the pre-computation time memory cost is acceptable for simulations on an average PC. Considering that in a surgical environment the number of the central operated organs is limited, the simulation speed for a single model is fast enough for modeling these deformable organs in real-time frame rate.

4.3. Robustness

Deformable models embedded in ODE dynamics simulators such as mass-spring model and FEM model usually suffer from the problem of instability. The robustness of the model cannot be guaranteed when the deformation is drastic or time step is large. In our hybrid model, because the global target positions of the mass particles in mass-spring simulator are computed by the BEM solver, which only depends on the boundary pressure condition and material properties. This can help our model to be stable in large time steps and to simulate some extreme deformations (Fig. 10).

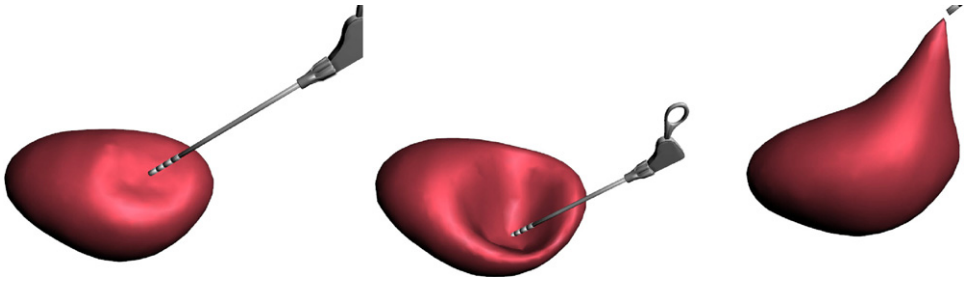

Fig. 10. Stable extreme large deformations of a kidney model interacting with a clipper.

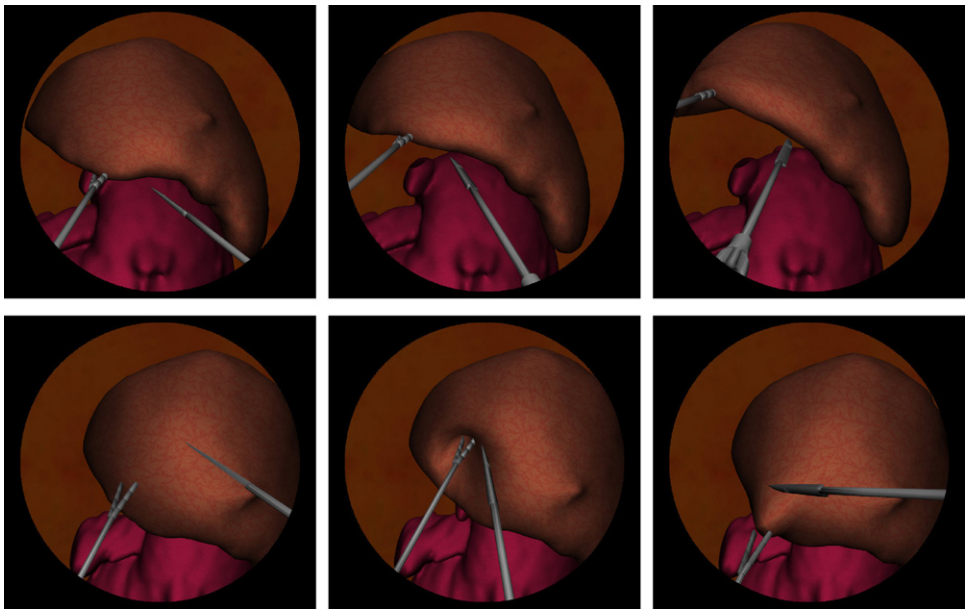

Fig. 11. Laparoscopic training by manipulating a clipper and a cutter on a liver model.

Although these deformations are not physical plausible and should never occur in a medical context, it is still important to guarantee the robustness of the model in such extreme cases.

4.4. Integration

The hybrid deformable model is integrated into a real-time virtual reality training system for laparoscopic surgery. Human organs with different material properties are modeled in a laparoscopic environment providing visually and haptically feedback. Surgeons are trained to perform operations in different surgical scenarios and acquire specific skills under different conditions. As illustrated in Fig. 11, trainee controls the clipper and cutter haptic devices with both hands, and interacts with the liver model and the kidney model under it to train respective surgical skills. In pictures in the first row, grabbling skills are trained by lifting the liver model using the clipper and touching the occluded tumor on the underneath kidney. In pictures in the second row, touching skills are trained by stabbing and dragging part of the liver to prepare for the cutting operations. The visual rendering, instrument controlling, deformable modeling, collision detection and haptic feedback are all computed in real-time with interactive frame rate.

5. Conclusion

In this paper we propose a new hybrid deformable model for real-time surgical simulation. Our model uses a BEM model to compute the global deformation and uses a mass-spring model to interactively model the dynamic behaviors of organs. The hybrid model is suitable for interactive surgical training applications, and provides visually accurate results in simulating the deformation of biological soft tissues with experimental inputs. Since our model is represented in a hybrid way including both surface meshes and discrete points, it is easy to couple the model with the point-based simulation framework [44,45]. Further work includes coupling the hybrid deformable model with other particle-based models such as SPH blood [41] to enhance the authenticity of the surgical scene and implementing the BEM solver in GPU to get better real-time performance.

Acknowledgments

We would thank all the group members of IGST for their valuable comments and suggestions. This paper was partially supported by the Chinese NSFC research fund (61190124) and the international research fund of STCSM (10440710600).

References

[1] Barbic J, James DL. Real-time subspace integration for St. Venant-Kirchhoff deformable models. ACM Trans Graphics (SIGGRAPH 2005) 2005;24(3):982–90.
[2] Bell N, Yu Y, Mucha PJ. Particle-based simulation of granular materials. In: SCA '05: proceedings of the 2005 ACM SIGGRAPH/eurographics symposium on computer animation. New York, NY, USA: ACM; 2005. p. 77–86.
[3] Brebbia CA, Telles JCF, Wrobel LC. Boundary element techniques: theory and applications in engineering. New York: Springer-Verlag; 1984.
[4] Chanthasopeephan T, Desai JP, Lau ACW. Modeling soft-tissue deformation prior to cutting for surgical simulation: finite element analysis and study of cutting parameters. #IEEE_J_BME# 2007;54(3):349–59.
[5] Chen X, Wechsler H, Pullen JM, Zhu Y, MacMahon EB. Knee surgery assistance: patient model construction, motion simulation, and biomechanical visualization'. IEEE Trans Biomed Eng 2001;48(9):1042–52.
[6] Chentanez N, Alterovitz R, Ritchie D, Cho L, Hauser KK, Goldberg K, et al. Interactive simulation of surgical needle insertion and steering. In: Proceedings of ACM SIGGRAPH 2009. 2009.
[7] Choi K-S, Soo S, Chung F-L. A virtual training simulator for learning cataract surgery with phacoemulsification. Comput Biol Med 2009;39(11):1020–31.
[8] Choi K-S, Sun H, Heng P-A. 'An efficient and scalable deformable model for virtual reality-based medical applications'. Artif Intell Med 2004;32(1):51–69.
[9] Hartmann F. Introduction to boundary elements: theory and applications. Berlin: Springer-Verlag; 1989.
[10] Fung YC. Biomechanics: mechanical properties of living tissues. 2nd ed. New York: Springer-Verlag; 1993.
[11] Hauser KK, Shen C, O'Brien JF. Interactive deformation using modal analysis with constraints. In: Graphics interface. A K Peters; 2003. p. 247–56.
[12] James DL, Pai DK. ArtDefo: accurate real time deformable objects. In: SIGGRAPH '99: proceedings of the 26th annual conference on computer graphics and interactive techniques. New York, NY, USA: ACM Press/Addison-Wesley Publishing Co; 1999. p. 65–72.
[13] James DL, Pai DK. DyRT: dynamic response textures for real time deformation simulation with graphics hardware. New York, NY, USA: ACM; 2002. p. 582–5.
[14] James DL, Pai DK. Multiresolution green's function methods for interactive simulation of large-scale elastostatic objects. ACM Trans Graph 2003;22(1):47–82.
[16] Kim J, Choi C, De Mandayam S, Srinivasan A. Virtual surgery simulation for medical training using multi-resolution organ models. Int J Med Rob Comp Assist Surg 2007;3(2):149–58.
[17] Keiser R. Meshless Lagrangian methods for physics-based animations of solids and fluids. ETH; 2006, doi:10.3929/ethz-a-005330494.
[18] Kenedi RM, Gibson T, Evans JH, Barbenel JC. Tissues mechanics. Phys Med Biol 1975;20(5):699–717.
[19] Lee T-Y, Sun Y-N, Lin Y-C, Lin L, Lee C. Three-dimensional facial model reconstruction and plastic surgery simulation. IEEE Trans Inf Technol Biomed 1999;3(3):214–20.
[20] Becker MM, Ihmsen MT. Corotated SPH for deformable solids. In: Proc. eurographics workshop on natural phenomena. 2009.
[21] Morris D, Sewell C, Blevins NH, Barbagli F, Salisbury K. A collaborative virtual environment for the simulation of temporal bone surgery. In: Barillot C, Haynor DR, Hellier P>, editors. MICCAI (2). Springer; 2004. p. 319–327.
[22] Müller M, Dorsey J, McMillan L, Jagnow R, Cutler B. Stable real-time deformations. In: SCA '02: proceedings of the 2002 ACM SIGGRAPH/eurographics symposium on computer animation. New York, NY, USA: ACM; 2002. p. 49–54.
[23] Müller M, Heidelberger B, Teschner M, Gross M. Meshless deformations based on shape matching. In: SIGGRAPH '05: ACM SIGGRAPH 2005 papers. New York, NY, USA: ACM; 2005. p. 471–8.
[24] Müller M, Keiser R, Nealen A, Pauly M, Gross M, Alexa M. Point based animation of elastic, plastic and melting objects. In: SCA '04: proceedings of the 2004 ACM SIGGRAPH/eurographics symposium on computer animation. Switzerland, Switzerland: Eurographics Association, Aire-la-Ville; 2004. p. 141–51.
[26] Müller M, Teschner M, Gross M. Physically based simulation of objects represented by surface meshes. In: Proc. Comput. Graph. Int. 2004. p. 156–65.
[27] Nealen A, Mueller M, Keiser R, Boxerman E, Carlson M. Physically based deformable models in computer graphics. Comp Graphics Forum 2006;25(4):809–36.
[28] Nesme M, Marchal M, Promayon E, Chabanas M, Payan Y, Faure F. Physically realistic interactive simulation for biological soft tissues. Recent Res Develop Biomech 2005;2:1–22.
[29] Sokhanvar S, Dargahi J, Packirisamy M. Hyperelastic modelling and parametric study of soft tissue embedded lump for MIS applications. Int J Med Rob Comput Assist Surg 2008;4(3):232–41.
[30] Crouch SL, Starfield AM. Boundary element methods in solid mechanics. London: Unwin Hyman Inc; 1990.
[31] Santhanam AP, Imielinska C, Davenport P, Kupelian P, Rolland JP. Modeling real-time 3D lung deformations for medical visualization. IEEE Trans Inf Technol Biomed 2008;12(2):257–70.
[32] Tahmasebi A, Hashtrudi-Zaad K, Thompson D, Abolmaesumi P. A framework for the design of a novel haptic-based medical training simulator. IEEE Trans Info Technol Biomed 2008;12(5):658–66.
[33] Harada T, Masayuki Tanaka SKYK. Real-time coupling of fluids and rigid bodies. In: APCOM '07 in conjunction with EPMESC XI. 2007.
[34] Teschner M, Heidelberger B, Mueller M, Pomeranets D, Gross M. Optimized spatial hashing for collision detection of deformable objects; 2003. p. 47–54.
[35] Teschner M, Heidelberger B, Muller M, Gross M. A versatile and robust model for geometrically complex deformable solids. In: CGI '04: proceedings of the computer graphics international. Washington, DC, USA: IEEE Computer Society; 2004. p. 312–9.
[38] Wang P, Becker AA, Jones IA, Glover AT, Benford S, Greenhalgh C, et al. A virtual reality surgery simulation of cutting and retraction in neurosurgery with force-feedback. Comput Methods Programs Biomed 2006;84(1):11–8.
[39] Wang P, Becker A, Jones I, Glover A, Benford S, Greenhalgh C, et al. Virtual reality simulation of surgery with haptic feedback based on the boundary element method. Comput Struct 2007;85(7–8):331–9.
[40] Li X, Gu L, Zhang S, Zhang J, Zheng G, Huang P, et al. Hierarchical spatial hashing based collision detection and hybrid collision response in a haptic surgery simulator. Int J Med Rob Comput Assist 2008;(4):77–86.
[41] Zaonyi J, Paget R, Szekely G, Grassi M, Bajka M. Real-time synthesis of bleeding for virtual hysteroscopy. Med Image Anal 2005;9(3):255–66.

[42] Zhang J, Gu L, Li X, Fang M. An advanced hybrid cutting method with an improved state machine for surgical simulation. Comput Med Imaging Graph 2009;33(1):63–71.
[43] Zhu B, Gu L, Zhang J, Yan Z, Pan L, Zhao Q. Simulation of organ deformation using boundary element method and meshless shape matching. In: Engineering in Medicine and Biology Society, 2008. EMBS 2008. 30th Annual International Conference of the IEEE. 2008. p. 3253–6.
[44] Zhu B, Gu L, Peng X, Zhou Z. A point-based simulation framework for minimally invasive surgery. In: Proc. of the 5th International Symposium on Computational Models for Biomedical Simulation. 2010. p. 130–8.
[45] Zhu B, Gu L, Zhou Z. Particle-based deformable modeling with pre-computed surface data in real-time surgical simulation. In: To appear in Proc. of 5th international workshop on medical imaging and augmented reality. 2010.